Spatial Inference of Traffic Transition Using Micro–Macro Traffic Variables

Suttipong Thajchayapong and Javier A. Barria, *Member, IEEE*

***Abstract*—This paper proposes an online traffic inference algorithm for road segments in which local traffic information cannot be directly observed. Using macro–micro traffic variables as inputs, the algorithm consists of three main operations. First, it uses interarrival time (time headway) statistics from upstream and downstream locations to spatially infer traffic transitions at an unsupervised piece of segment. Second, it estimates lane-level flow and occupancy at the same unsupervised target site. Third, it estimates individual lane-level shockwave propagation times on the segment. Using real-world closed-circuit television data, it is shown that the proposed algorithm outperforms previously proposed methods in the literature.**

***Index Terms*—Freeway segments, microscopic traffic variables, spatial inference, traffic anomalies, traffic estimation.**

I. Introduction

PROMPT dissemination of vehicular traffic information is essential to traffic management center personnel, so that appropriate and proactive actions are taken to neutralize any undesirable evolution of the underlying traffic condition. However, due to cost and topographic limitations, it may not be feasible to deploy sensors on every road segment. Furthermore, operation managers could also encounter a sensor or group of sensors out of service and/or malfunctioning. Therefore, developing spatial inference algorithms to operate where traffic variables cannot be directly measured is of great help to traffic managers and operators as they could continue to operate at almost the same levels of confidence prior to the onset of an outage period.

The majority of previously proposed traffic forecast and estimation models has been developed under an assumption that traffic variables are locally available at the location of interest [5]–[7]. On the other hand, a relatively fewer number of recent models have been designed for spatial inference on road segments where local information is not available [4], [8]–[11]. Many of these models are primarily designed for seasonal/cyclic traffic transitions (e.g., routine patterns on weekdays [4]), but they have not been explicitly tested with unexpected traffic transitions (e.g., an onset of incident [3], [12], [13]), which can be crucial in real-world operations.

In this context, the ability to incorporate both macroscopic and microscopic traffic variables is also essential as they can provide complementary information for spatial inference models. Macroscopic traffic variables capture aggregate behaviors of vehicles, whereas microscopic traffic variables describe individual vehicle behaviors and their interactions [12], [13]. However, most of the previously proposed spatial inference models [4], [8]–[11] incorporate mainly macroscopic traffic variables, which cannot capture changes in microscopic-level characteristics.

Recently, it has been reported in [14] that while a prediction model based on Newell's kinematic wave theory [2] performs very well in heavy-traffic conditions, the model can underperform under sporadic congestion or light-traffic conditions. This finding highlights the increasing interest for real-time monitoring algorithms under a nearly congested situation and low flow conditions [2], [3]. Furthermore, we note that there has been an increasing interest in investigating lane-level vehicular traffic behavior by the transportation research community [12], [13], [15]–[18]. In this context, closed-circuit television (CCTV) traffic detectors have gained popularity, as they are reported to be more cost effective and less prone to damage than loop detectors [2]–[4]. CCTV cameras can also provide reliable traffic measurements during free-flow and light-traffic conditions [19], which are very useful for the type of algorithms we are presenting in this paper as it is based on learning underlying rules to classify different traffic transitions. Furthermore, since traffic transition can occur outside the sensor coverage range (e.g., CCTV camera view) and/or sensors information could become unavailable due to their associated repair/restoration time, there is the need to develop novel algorithms that can overcome such transient or permanent loss of fixed monitoring positions to enable a nearly seamless operation under these suboptimal conditions.

The contributions of this paper can be summarized as follows: An online algorithm is designed to use both microscopic (variability of interarrival time) and macroscopic (flow, occupancy, and average speed) traffic variables for spatial inference, which consists of three operations. First, it spatially infers traffic transitions at an unsupervised target location, in between two adjacent fixed CCTV camera sensor locations, where traffic information cannot be directly measured. Second, the algorithm estimates lane-level flow and occupancy at the same unsupervised target location, which is in a much finer scale than previous approaches [4]. Third, the proposed algorithm performs online estimation of lane-level shockwave propagation time by

Manuscript received November 1, 2013; revised May 12, 2014; accepted July 21, 2014. Date of publication September 9, 2014; date of current version March 27, 2015. The Associate Editor for this paper was R. Liu.

S. Thajchayapong is with the National Electronic and Computer Technology Center (NECTEC), National Science and Technology Development Agency (NSTDA), Pathumthani 12120, Thailand.

J. A. Barria is with the Department of Electrical and Electronic Engineering, Imperial College London, London SW7 2AZ, U.K. (e-mail: j.barria@imperial.ac.uk).

Color versions of one or more of the figures in this paper are available online at http://ieeexplore.ieee.org.

Digital Object Identifier 10.1109/TITS.2014.2345742

assessing temporally local correlation samples of upstream and downstream speeds.

This paper proposes an enhanced version of the algorithm in [18], which is designed for spatially inferring both normal and anomalous traffic transitions. This paper is organized as follows. Section II reviews related work. Section III describes the framework of this study. The proposed algorithm is presented in Section IV, and evaluation results are discussed in Section V. Finally, Section VI presents final remarks and future work.

II. Related Work

During the past few years, various short-term traffic forecast and estimation models have been proposed [5], whereas the most recent efforts have been focused on improving prediction accuracy and computational efficiency [6], [20], [21] and reducing computational complexity [7]. However, the majority of these models has been developed under a common assumption that traffic variables can be directly obtained at the location of interest.

Relatively much fewer number of studies have been proposed to operate on road segments where local information cannot be directly measured, and they are not primarily designed to be adaptable to unexpected or anomalous traffic transitions [4], [8]–[11]. Kalman filter (KF)-based approaches have been shown to have advantages over other methods for online estimation of traffic flows. In [4], a KF-based model is used as an underlining tool to capture spatial and temporal evolutions of traffic flows on adjacent sites. However, the assessment in [4] is conducted only with aggregated traffic flows on weekdays, which follow routine patterns. A recently proposed traffic surveillance system in [8] also uses an extended KF (EKF) model to estimate traffic flow and speed on the A3 freeway in Italy. However, the proposed EKF model is designed for aggregated road-level estimation, and the evaluations were conducted with only two days of traffic data, and the estimation accuracy has not been numerically assessed [e.g., with mean absolute percentage error (MAPE)]. In [9], a context awareness (e.g., time of day and weather data) model is proposed to infer traffic congestion levels on road segments, but basic lane-level traffic variables are not available.

Furthermore, the majority of previous works has not been developed for lane-level inference as their focus is at a more coarse-grained level, e.g., at road-level [4], [8], [9], zone-level [10], or even city-level [11]. A family of geostatistical interpolation techniques called ordinary kriging [22] has been extensively used to spatially and collectively infer zonal traffic conditions over a large area consisting of several road segments. In [11], the focus is on a long-term inference of annual average daily traffic flow between the cities across the state of Texas. Similarly, ordinary kriging is employed over a fixed time duration to spatially infer traffic congested areas consisting of several road segments in [10]. Although the studies in [10] and [11] are particularly useful for transportation planning and policy making at the zonal level, their proposed models cannot be applied for spatial inference and estimation at lane-level, which is in a much finer scale. Furthermore, the approach in [10] is only tested with traffic data collected during rush hours, which follow routine patterns, and there is no explicit validation between the inferred and the measured values. Unlike previous models, the algorithm developed in this paper focuses on the inference of normal and anomalous traffic transitions, lane-level estimations of traffic variables, and shockwave propagations.

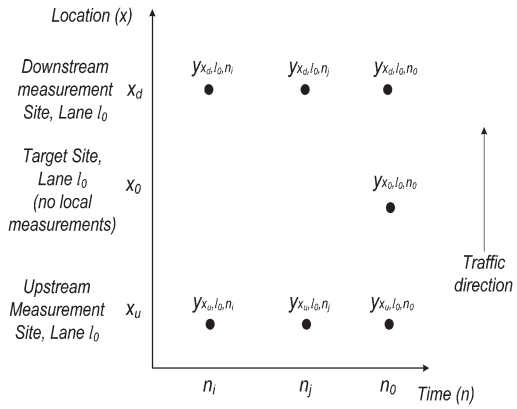

Fig. 1. Measurement and target sites over a space–time diagram.

With respect to the inputs used to assess traffic transition, the majority of the previously proposed short-term forecast and estimation models only uses macroscopic traffic variables, which are likely to miss anomalous traffic transitions associated with individual transient behaviors of vehicles that can occur under nonrecurring circumstances (e.g., accidents) [5], [12], [13]. Unlike the majority of the previously proposed models, the algorithm proposed in this paper is also designed to infer traffic condition transition by assessing statistics of interarrival time, which are microscopic traffic variables.

III. Analysis Framework

As shown in Fig. 1, the aim is to infer traffic transition and to estimate a traffic variable y_{x_0,l_0,n_0} on lane l_0, at time n_0 and location x_0 referred to as *target site*. Only the measurements from adjacent sites $\{x_u, x_d\}$, referred to as *measurement sites*, would be used as input that could be measured over space at the time of inference, e.g., y_{x_u,l_0,n_0}, y_{x_d,l_0,n_0}, and/or at previous time steps, e.g., y_{x_u,l_0,n_i}, y_{x_u,l_0,n_j}, y_{x_d,l_0,n_i}, and y_{x_d,l_0,n_j}. Local measurements at the target site x_0 are not used in either the inference of traffic transition or the estimation of y_{x_0,l_0,n_0}. It is also assumed that vehicle travel time and shockwave propagation time are not known *a priori*.

The focus of the proposed algorithm is on inferring transition between free-flow and congested conditions [23] using information from upstream and downstream measurement sites. Traffic transitions are classified into *free-flow*, *congested*, *transient anomaly*, and *lane blocking*. Free-flow and congested transitions refer to an onset when traffic starts to evolve to free-flow and congested conditions, respectively. Transient anomaly refers to a transition associated with temporarily minor disruptions of traffic flow (e.g., a distraction on a freeway shoulder), whereas lane blocking refers to a transition associated with major disruptions (e.g., an accident or a disable vehicle that blocks lanes) [12], [13]. As transient anomaly and lane blocking

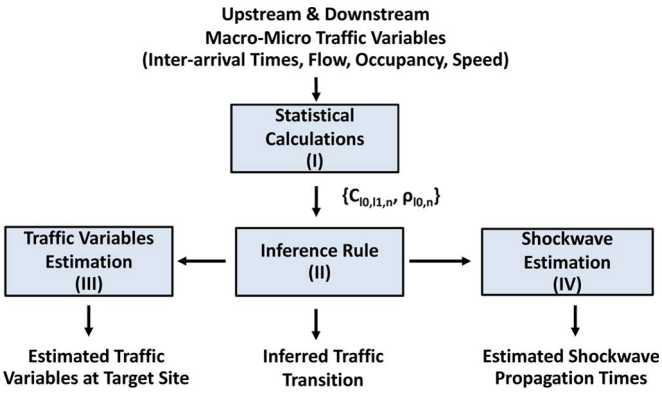

Fig. 2. Proposed algorithm.

are nonrecurring in nature, they usually cannot be inferred by seasonal/cycilc components used in previously proposed models [4], [10], [11].

Estimating lane-level *flow* and *occupancy* is also important as they can further provide fine-scale information for other road traffic monitoring applications, for example, to calculate vehicle density or to anticipate future traffic transition [5]. As the algorithm developed in this paper is meant to support the operation of fixed sensor, *flow* is defined as the rate of vehicles passing a point during a given time interval as in HCM [24], which is a special case of Edie's for a point in space [25]. *Occupancy* refers to a fraction of time that a designated position is occupied by vehicles. Finally, *shockwave* is defined as moving speed drop areas as in [26].

IV. Proposed Inference Algorithm

A. Overview of the Algorithm

The proposed algorithm operates as shown in Fig. 2. First, spatial covariance of interarrival time $C_{l_0,l_1,n}$ and the difference of lane-level standard deviations of interarrival time $\rho_{l_0,n}$ are calculated in Block I, which are then used to infer traffic transition at the target site in Block II. The schemes used in Blocks I and II are described in detail in Section IV-B. The inferred transition is then used by the estimation model in Block III to select a weighting factor to estimate flow and occupancy at the target site x_0. The scheme used to select $a_{l_0,n}$ in Block III is described in detail in Section IV-D, whereas the estimation model is described in Section IV-C. Finally, if a congested transition is inferred, the proposed algorithm estimates shockwave propagation times in Block IV, which is described in Section IV-F.

B. Inference Rule

An important element of the proposed algorithm is the inference rule, which is used to infer traffic transitions and to select an appropriate weighting factor $a_{l_0,n}$ (to estimate traffic variables in Section IV-C) by assessing only spatial and temporal variations of interarrival time. The inference rule uses two microscopic statistics: 1) spatial covariance of interarrival time $C_{l_0,l_1,n}$ and 2) the difference of lane-level standard deviations of interarrival time $\rho_{l_0,n}$, which are calculated as in (1) and (2), respectively, where l_1 denotes a lane adjacent to l_0, $\underline{Y}_{l_0,n}=[y_{x_d,l_0,n-L},\ldots,y_{x_d,l_0,n},y_{x_u,l_0,n-L},\ldots,y_{x_u,l_0,n}]$, $\underline{Y}_{l_1,n}=[y_{x_d,l_1,n-L},\ldots,y_{x_d,l_1,n},y_{x_u,l_1,n-L},\ldots,y_{x_u,l_1,n}]$, and $s_{l_0,n}$ and $s_{l_1,n}$ are the standard deviations of $\underline{Y}_{l_0,n}$ and $\underline{Y}_{l_1,n}$, respectively. The spatial covariance $C_{l_0,l_1,n}$ is used to measure the correlation of variation of interarrival time on adjacent lanes as well as the spatial variations between upstream and downstream interarrival times, whereas $\rho_{l_0,n}$ is used to measure difference in lane-level variations between adjacent lanes. We note that the calculations of $C_{l_0,l_1,n}$ and $\rho_{l_0,n}$ include upstream and downstream input samples at the same time to simplify the online implementation of operating the inference rule, traffic variable estimation, and shockwave estimation together online, as shown in Fig. 2. Note that calculating input sample differences at different times would require specific knowledge on vehicle travel time and shockwave propagation time, which are not known *a priori*. Thus

$$C_{l_0,l_1,n}=E\left[\left(\underline{Y}_{l_0,n}-E\left[\underline{Y}_{l_0,n}\right]\right)\left(\underline{Y}_{l_1,n}-E\left[\underline{Y}_{l_1,n}\right]\right)^T\right] \quad (1)$$

$$\rho_{l_0,n}=\frac{s_{l_1,n}-s_{l_0,n}}{s_{l_0,n}}. \quad (2)$$

The method for deriving the inference rule is shown in Fig. 3, which is based on a conventional *overfit-and-simplify* approach [27]. The inference rule derivation takes as input a historical data set that consists of interarrival times measured at upstream and downstream measurement sites and an independent log of traffic conditions and incident cases. An initial rule set is derived, which consists of a set of conditions for inferring traffic transition by assessing the values of $C_{l_0,l_1,n}$ and $\rho_{l_0,n}$, i.e., {IF $C_{l_0,l_1,n}>C_I$ and $\rho_{l_0,n}>\rho_I$, THEN free-flow at target site; ELSE IF $C_{l_0,l_1,n}<C_I$ and $C_{l_0,l_1,n}>C_{II}$, THEN congested at target site;. . ..}, where C_I, C_{II}, and ρ_I are obtained from historical data. As conditions of $C_{l_0,l_1,n}$ and $\rho_{l_0,n}$ associated with a certain traffic transition may be overlapped with another traffic transition, the next step is to remove redundant and/or overlapping conditions. Each simplified version of the rule set is validated with the log of traffic conditions and incident cases. This simplification is performed until the inference error can no longer be reduced. The derived inference rule is then used in Block II in Fig. 2.

Free-flow and congested traffic transitions are primarily inferred by assessing the value of $C_{l_0,l_1,n}$. The value of $|C_{l_0,l_1,n}|$ can be large, particularly under free-flow conditions because there is a high probability of large durations between consecutive arrivals of vehicles, and the arrivals of vehicles on one lane can be more frequent than the arrivals on an adjacent lane. As the number of vehicles increases toward congestion, interarrival times on each lane are reduced and much more consistent with adjacent lanes, which would subsequently reduce $C_{l_0,l_1,n}$.

Nonrecurring circumstances associated with transient anomalies and lane blockings can also be captured using $C_{l_0,l_1,n}$ and $\rho_{l_0,n}$ as the variations of interarrival time on adjacent lane change [13]. Lane blockings are likely to increase $C_{l_0,l_1,n}$ and $\rho_{l_0,n}$ as changes in interarrival time on adjacent lanes are highly correlated at both upstream (e.g., vehicles queue up) and downstream (e.g., vehicles discharge) sites.

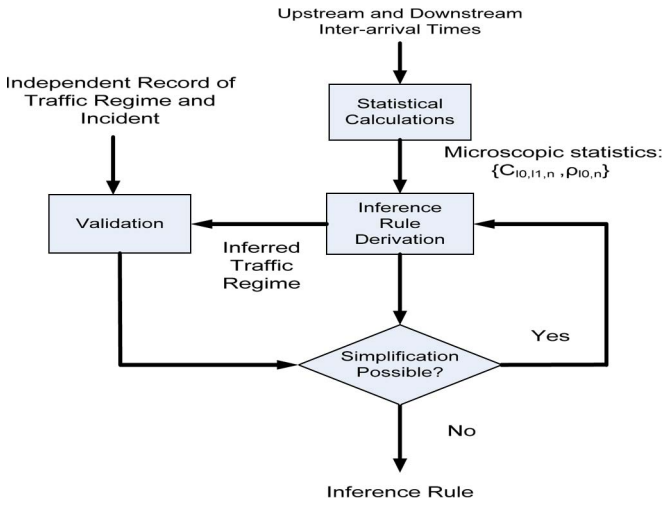

Fig. 3. Derivation of inference rule to be used in Block II of the proposed algorithm in Fig. 2.

On the other hand, transient anomalies associated with minor disruptions (e.g., distractions on the shoulder [12], [13]) are less likely to cause significant differences between the upstream and downstream interarrival times, which would reduce the difference in the variation of interarrival times on adjacent lane and subsequently reduce $\rho_{l_0,n}$.

C. Estimation of Traffic Variables

To capture the variability according to the change in traffic variables over both time and space, the estimation model shown in (3) is proposed, which incorporates the spatial and temporal difference between the upstream and downstream measurement sites. Thus

$$\hat{y}_{x_0,l_0,n} = \hat{y}^{\text{krig}}_{x_0,l_0,n} + a_{l_0,n}\frac{1}{L}\sum_{m=n-L}^{n}(y_{x_d,l_0,m} - y_{x_u,l_0,m}) + \beta_{x_0,l_0,n}. \quad (3)$$

In this model, the first term $\hat{y}^{\text{krig}}_{x_0,l_0,n}$ is the estimated value at the target site x_0 on lane l_0 at time n obtained from applying ordinary kriging [22] to interpolate data from the measurement sites. As ordinary kriging does not incorporate the spatial variability of the traffic variables among the measurement sites themselves, the second term in (3) is incorporated to capture spatial variability under different traffic conditions. The second term consists of $y_{x_d,l_0,m}$ and $y_{x_u,l_0,m}$, which are the traffic variables measured at the downstream and upstream measurement sites on lane l_0, respectively. We note that the proposed model only uses temporal samples from adjacent measurement sites from previous time steps $n-L$ up to n. Our approach is intended to work online; hence, future samples (e.g., at $n+1$, $n+2,\ldots$) would not be available while operating at time step n. The weighting factor $a_{l_0,n}$ is used to scale the upstream–downstream difference $(y_{x_d,l_0,n} - y_{x_u,l_0,n})$, where the selection of $a_{l_0,n}$ is described in detail in Section IV-D.

The third term $\beta_{x_0,l_0,n}$ is used to incorporate seasonal and/or cyclic patterns of individual traffic variables at particular times. The aim is to enable the model to be applicable on road segments, which undergoes particular seasonal and/or cyclic patterns, e.g., recurring traffic congestion during morning rush hours.

D. Selection of Weighting Factor $a_{l_0,n}$

Here, we introduce a method to select $a_{l_0,n}$, which is then used in the estimation model (Block III in Fig. 2). Based on the historical data set, $a_{l_0,n}$ is selected according to the inferred traffic transition from Block II in Fig. 2, the type of traffic variables to be estimated, and the value of $\rho_{l_0,n}$. The selection of $a_{l_0,n}$ is based on the expected correlation between the variations at measurement sites and at the target site, which depends on the inferred traffic transition.

In addition, an upper bound should be determined for $a_{l_0,n}$ to prevent overestimation because the standard deviation difference $\rho_{l_0,n}$ itself can sometime be unusually high due to transient behavior of individual vehicles (e.g., temporarily excessive speed). This upper bound is dependent on traffic characteristics of the road segment as well as the inferred traffic transition and should be empirically determined based on the historical data set.

E. Selection of Time Step

The selection of time step for forecasting and estimation is very important as shorter time steps can exhibit higher variability, which can undermine the accuracy of forecasting and estimation models. Although the 15-min interval is often recommended [6] to avoid strong fluctuation at shorter intervals, using a step as low as a 5-min interval can provide more fine-grained information. In this paper, the estimation is performed in a step of 5-min interval, which is also the shortest forecasting and estimation step used in practice [5]. We note that some previous work such as [28] have used 2-min intervals.

F. Estimation of Shockwave Propagation Time

This section describes the shockwave estimation, which is implemented in Block IV in Fig. 2. The aim is to find $\tau_n^{\max}$, which is the time lag that gives maximum cross-correlation between upstream and downstream average speeds[1] at time step n. Consecutive nonzeros $\tau_n^{\max}$ would signify the occurrence of a shockwave front as upstream and downstream average speeds are correlated with time lags greater than zero (a shockwave front cannot possibly have a zero propagation time between two sites). Then, the shockwave propagation time is estimated as the average of these consecutive nonzeros $\tau_n^{\max}$.

Coifman and Wang [15] proposed a method to find $\tau_n^{\max}$, by calculating cross-correlation coefficients between time series of average speed measured at downstream and upstream sites.

[1]Speed refers to the motion of traffic as it travels downstream, and local speed is the measurement at the location of a sensor. Velocity refers to the backward motion of shockwave [15].

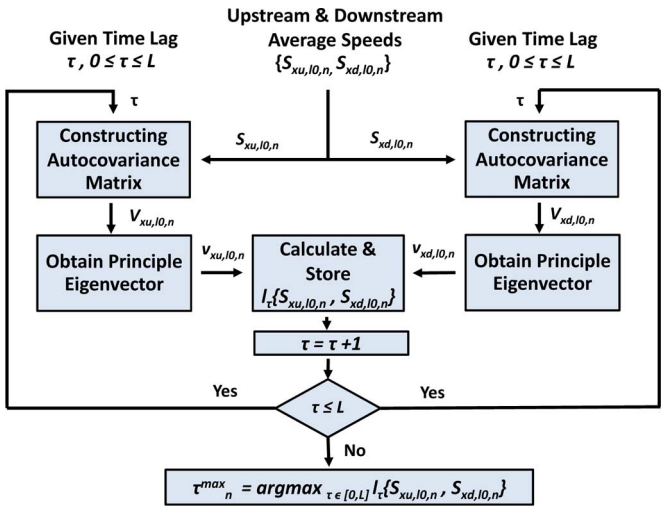

Fig. 4. Shockwave propagation time estimation implemented in Block IV of the proposed algorithm in Fig. 2.

However, using only cross-correlation coefficients may not be able to capture complex, nonlinear, and/or nonstationary relationships between local speed patterns at two different locations. Such relationship may also vary at different times. Therefore, an improved method is needed.

To find $\tau_n^{\max}$, we modify a local correlation tracking previously proposed in [29], which generalizes the linear cross-correlation by comparing spectral decompositions of local autocovariance matrices of two time series. To capture similarity of local average speed patterns, LoCo score [29] with time lag τ: $l_\tau\{S_{x_u,l_0,n}, S_{x_d,l_0,n}\}$ is calculated as shown in (4), where τ denotes time lag. $S_{x_u,l_0,n}$ and $S_{x_d,l_0,n}$ denote vectors of upstream and downstream average speeds measured on lane l_0 at time step n, respectively. $V^T_{S_{x_u,l_0,n}}$ denotes a transpose of an autocovariance matrix $V_{S_{x_u,l_0,n}}$, and $v_{S_{x_u,l_0,n}}$ denotes the principle eigenvector of an autocovariance matrix $V_{S_{x_u,l_0,n}}$. Thus

$$l_\tau\{S_{x_u,l_0,n}, S_{x_d,l_0,n}\} = \frac{1}{2}\left(\left\|V^T_{S_{x_u,l_0,n}} v_{S_{x_d,l_0,n}}\right\| + \left\|V^T_{S_{x_d,l_0,n}} v_{S_{x_u,l_0,n}}\right\|\right). \quad (4)$$

As shown in Fig. 4, for each time step n and a given sliding window size L, lane-level upstream average speeds $S_{x_u,l_0,n} = [s_{x_u,l_0,n-L}, \ldots, s_{x_u,l_0,n-1}, s_{x_u,l_0,n}]$ and downstream average speeds $S_{x_d,l_0,n} = [s_{x_d,l_0,n-L}, \ldots, s_{x_d,l_0,n-1}, s_{x_d,l_0,n}]$ are obtained from the sensors. For each value of τ, local upstream and downstream autocovariance matrices $V_{S_{x_u,l_0,n}}$, $V_{S_{x_d,l_0,n}}$ are constructed, where $V_{S_{x_u,l_0,n}} = E[(S_{x_u,l_0,n} - m_{x_u,l_0,n})(S_{x_u,l_0,n} - m_{x_u,l_0,n})^T]$, $V_{S_{x_d,l_0,n}} = E[(S_{x_d,l_0,n} - m_{x_d,l_0,n})(S_{x_d,l_0,n} - m_{x_d,l_0,n})^T]$, and $m_{x_u,l_0,n}$ and $m_{x_d,l_0,n}$ are the means of $S_{x_u,l_0,n}$ and $S_{x_d,l_0,n}$, respectively. Then, the principle eigenvectors $v_{S_{x_u,l_0,n}}$ and $v_{S_{x_d,l_0,n}}$ of upstream and downstream autocovariance matrices are obtained. A LoCo score $l_\tau\{S_{x_u,l_0,n}, S_{x_d,l_0,n}\}$ is then calculated using (4). The process is repeated online for all values of $\tau \in [0, L]$ to find the value of $\tau_n^{\max}$ that gives maximum $l_\tau\{S_{x_u,l_0,n}, S_{x_d,l_0,n}\}$.

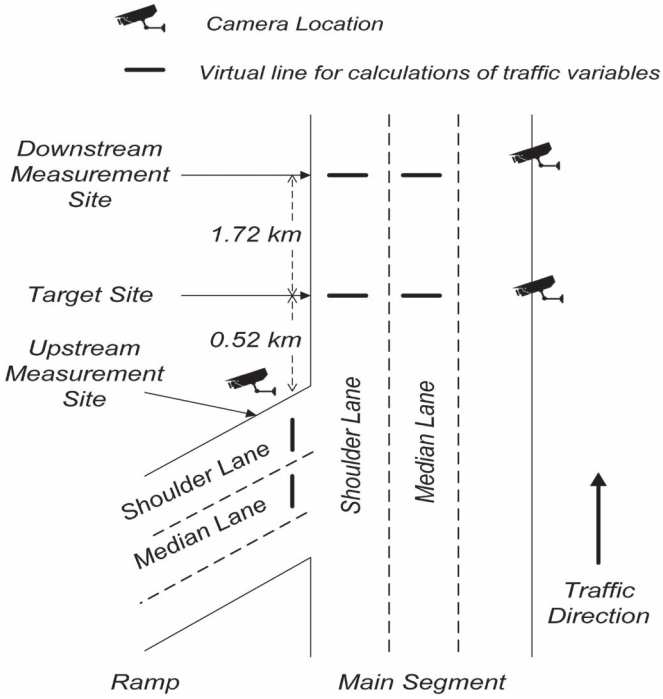

Fig. 5. Sketch of expressway segment where real-world data were obtained.

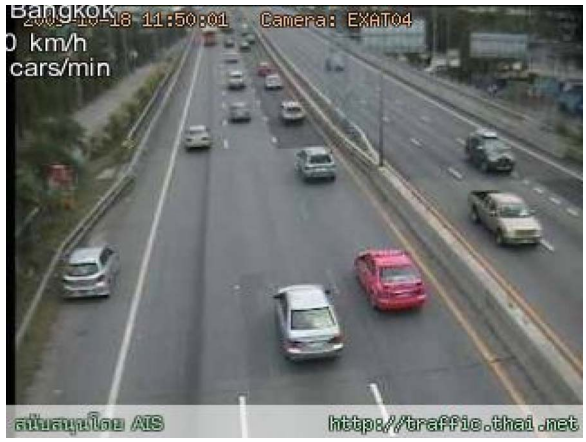

Fig. 6. Video snapshot from a camera at the target site.

V. Performance Evaluation Using Real-World Data

A. Descriptions of the Data

In order to assess proposed algorithm, a real-world data set was recorded by cameras mounted on an urban expressway segment in Bangkok, Thailand. These cameras have been previously installed and are operated by the Bangkok Expressway Public Company (BECL). As shown in Fig. 5, the upstream and downstream cameras are approximately 0.52 and 1.72 km from the camera mounted at the target site. Recurrent congestion occurs during morning rush hours on weekdays when commuters are traveling into the city. Traffic incidents are recorded by BECL. A video snapshot from a camera at the target site is shown in Fig. 6. The aim is to infer traffic transitions and then estimate flow and occupancy at the target site using traffic data from adjacent measurement sites, whereas

traffic variables obtained by cameras at the target site itself are used for validation. It is also important to note that at the upstream measurement site, traffic from the main segment is merged with traffic from a ramp; however, only traffic data from the ramp are available, whereas traffic data on the main segment are unknown.

Each camera is capable of detecting individual vehicles that passed the expressway segment. On the image frame of each camera, a virtual line was drawn on the location of interest [17]. For a vehicle i, t^{in} was recorded, where t_i^{in} is the time that the vehicle crossed the virtual line. An interarrival time observed by vehicle i to its leading vehicle $i-1$ is calculated as $t_i^{\text{in}} - t_{i-1}^{\text{in}}$. For a given time period L, flow is set equal to the number of vehicle arrivals to the virtual line. Occupancy is calculated as $(\sum_{i=1}^{\eta} o_i/L) \times 100$, where o_i is the duration that a vehicle i was present on the virtual line. Furthermore, for evaluation purposes, traffic conditions and incidents that took place are independently and manually logged by a team of transportation researchers, using video images from the camera at the target site, and incident reports from BECL.

The real-world data set used in this paper was collected by the cameras under different traffic conditions daily from 6 A.M. to 6 P.M. for a one-month period in October 2009. The average number of vehicles detected passing the freeway segment is found to be approximately 50 000 vehicles per day; hence, there are approximately 1 550 000 records for the one-month period of data collection. A cross-validation technique is used to assess the proposed algorithm where the real-world data set is separated into training and testing sets.

B. Derivation of Inference Rule Based on Real-World Data

Applying the methods in Section IV-B and D offline to the training set consisting of one week of data, two cases of transient anomalies, and two cases of lane blockings, we obtain the following inference rule:

IF $(C_{l_0,l_1,n} < 0) \vee (C_{l_0,l_1}, n > 0.5)$; Free-flow
IF(estimating time occupancy); $a_{l_0,n} = 0$;
IF(estimating traffic flow); $a_{l_0,n} = 1 - \rho_{l_0,n}$;
IF $(0 \leq C_{l_0,l_1,n} \leq 0.5)$; Congested
IF(estimating time occupancy); $a_{l_0,n} = min(\rho_{l_0,n}, 2.5)$;
IF(estimating traffic flow); $a_{l_0,n} = min(\rho_{l_0,n}, 1)$;
IF $(C_{l_0,l_1,n} > 5) \wedge (\rho_{l_0,n}, n > 2.5)$; Lane blocking
IF(estimating time occupancy); $a_{l_0,n} = \rho_{l_0,n}$;
IF(estimating traffic flow);
$a_{l_0,n} = \rho_{l_0,n} \cdot 1_{\triangle y_{l_0,n} > \triangle y_{l_1,n}} + (\rho_{l_0,n} - 1) \cdot 1_{\triangle y_{l_0,n} \leq \triangle y_{l_1,n}}$;
IF $(\rho_{l_0,n}, n \leq 2.5)$; Transient Anomaly
IF(estimating time occupancy); $a_{l_0,n} = min(\rho_{l_0,n}, 2)$;
IF(estimating traffic flow); $a_{l_0,n} = min(\rho_{l_0,n}, 1)$;

This inference rule is then applied to the testing set as if it is being operated online, where each inference operation is performed per time step n. The conditions for assessing the values of $C_{l_0,l_1,n}$ and $\rho_{l_0,n}$ in the inference rule may change if the sensors' locations are changed.

We note that for flow under lane blockings, the choice of $a_{l_0,n}$ primarily depends on whether traffic disruption is more likely to occur on the current lane of interest in respect to an adjacent lane. This likelihood of having an onset of traffic disruption can be assessed by comparing the difference in upstream and downstream traffic flows on the current lane $\triangle y_{l_0,n} = (1/L) \sum_{m=n-L}^{n} (y_{x_d,l_0,m} - y_{x_u,l_0,m})$ with that of an adjacent lane $\triangle y_{l_1,n} (1/L) \sum_{m=n-L}^{n} (y_{x_d,l_1,m} - y_{x_u,l_1,m})$. Higher difference in upstream and downstream traffic flows indicates higher probability that the traffic is disrupted on the lane of interest and that the estimated traffic flow at the target site should be proportionally set to $\rho_{l_0,n}$, i.e., $a_{l_0,n} = \rho_{l_0,n}$. In contrast, if traffic disruption is more likely on an adjacent lane, the estimated traffic flow at the target site should still be proportional, but at a slower rate, to $\rho_{l_0,n}$ as it is more likely that vehicles have more incentives to change to the current lane, that is, $a_{l_0,n} = \rho_{l_0,n} - 1$.

C. Benchmark Algorithms for Comparisons

To assess the capabilities of the proposed algorithm to infer traffic transitions, the dual-station algorithm [3] is employed as benchmark. This algorithm is selected primarily because it is similar to the framework of our proposed algorithm. First, its rule-based approach is particularly designed to operate online with a camera-based detector system. Second, its target is to infer traffic transitions due to lane blocking using flow, speed, and occupancy measured at upstream and downstream sites. Third, this algorithm has been shown to perform well under real-world scenarios on Singapore's expressway [3].

For the estimation of traffic variables, the three-detector algorithm based on Newell's simplified kinematic wave model is used as a benchmark [1], [2]. This algorithm is particularly efficient for online estimation as Newell's simplified model [2] does not pose any particular requirement on segment length and, subsequently, does not consume much computational resources. Furthermore, it has been shown that this algorithm has potential to improve the estimation accuracy of flow [1].

KF-based algorithms are also employed as benchmarks for estimation of traffic variables. This type of algorithm has been originally proposed in [30] and has also been recently assessed in [4] and [8] in terms of its ability to improve accuracy in traffic flow estimation at locations where traffic data cannot be directly measured. Two KF-based estimation algorithms, i.e., KF-1 and KF-2, are employed as benchmarks. KF-1 operates where local measurements are missing at the target site, whereas KF-2 operates under an ideal scenario where it can use traffic variables from both adjacent measurement and target sites to adjust the estimation accuracy. The purpose of including KF-2 as a benchmark is to assess how well the proposed algorithm performs with respect to an ideal scenario where data from the target site can be used for estimation.

D. Results and Discussions on the Inference of Traffic Transitions

We first note that the accuracy reported in this experiment is generally lower than in previous studies due to the following

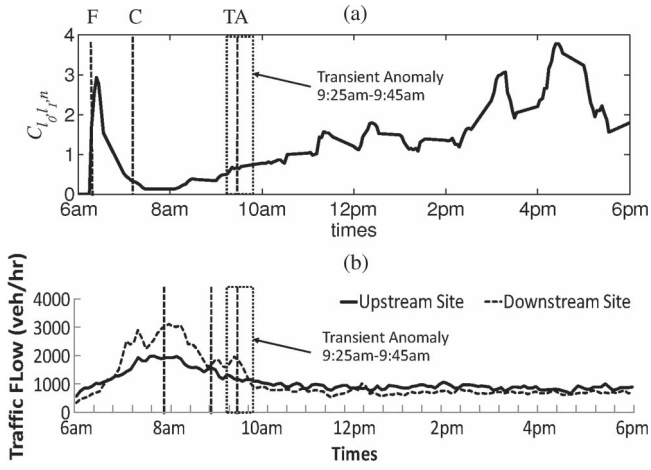

Fig. 7. Inferring traffic transition on October 12, 2009 using (a) the proposed algorithm and (b) the dual-station algorithm [3]: F, C, and TA denote free-flow, congested, and transient anomaly, respectively.

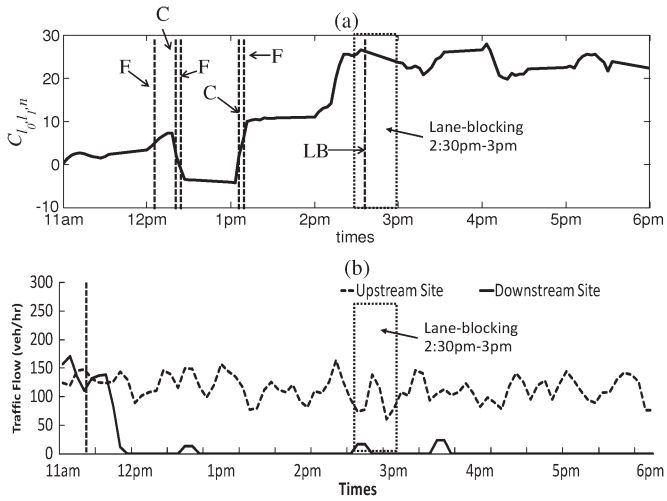

Fig. 8. Inferring traffic transition on October 18, 2009 using (a) the proposed algorithm and (b) the dual-station algorithm [3]: F, C, and LB denote free-flow, congested, and lane blocking, respectively.

reasons. First, the algorithms are assessed where traffic transitions are usually not known in advance. Second, this is a lane-level estimation, which is generally more prone to errors than aggregated estimations [4]. Third, this experiment is conducted on nonhomogenous road segments where input information is only partially available. The temporal samples of upstream measurements are used as input in the proposed algorithm, as well as in benchmark algorithms. Therefore, the partial availability of upstream data affect the accuracy of all the algorithms.

As shown in Fig. 7(a), at approximately 6:15 A.M., free-flow transition (point F and vertical dotted line) is first inferred. Then, as traffic demand continues to increase toward morning rush hour and exceeds the capacity of the expressway segment at approximately 7:15 A.M., congested transition (point C and vertical dotted line) is inferred by the proposed algorithm. These traffic transitions inferred by the proposed algorithm closely match those independently logged by transportation researchers using video images from the camera at the target site. On the other hand, as shown in Fig. 7(b), the dual station misses these transitions.

Moreover, the proposed algorithm can infer transient anomaly [point TA and vertical dotted line in Fig. 7(a)], which was recorded at approximately 9:25–9:45 A.M. on October 12, 2009. This transient anomaly corresponds to a locally minor disruption at the target site, which occurred while there are a substantial number of vehicles on the expressway segment. The dual-station algorithm can also infer this transient anomaly, as shown in the dotted vertical lines in Fig. 7(b). This is primarily because the dual-station algorithm is designed to operate under moderate- and heavy-traffic flow.

The proposed algorithm and the dual-station algorithm are further assessed under lane blocking, which was recorded at approximately 2:30–3:00 P.M. on October 18, 2009, as shown in Fig. 8. It can be seen that the proposed algorithm can infer this lane blocking as shown Fig. 8(a), whereas the dual-station algorithm misses this same lane blocking as shown Fig. 8(b). This lane blocking is associated with a disabled vehicle that caused most of the vehicles to avoid the shoulder lane and use the middle and right lanes. Consequently, flow measured on the shoulder lane at the downstream site is not large enough to trigger the dual-station algorithm.

TABLE I
MAPE FROM ESTIMATING TRAFFIC VARIABLES, EVERY 5 MINS, USING REAL-WORLD DATA

Proposed Algorithm (no local measurements)	MAPE on Shoulder Lane	MAPE on Median Lane
Flow	0.213	0.139
Occupancy	0.441	0.221
Three-detector [1, 2] (no local measurements)	MAPE on Shoulder Lane	MAPE on Median Lane
Flow	0.544	0.187
KF-1 (no local measurements)	MAPE on Shoulder Lane	MAPE on Median Lane
Flow	0.307	0.527
Occupancy	0.703	0.511
KF-2 (with local measurements)	MAPE on Shoulder Lane	MAPE on Median Lane
Flow	0.122	0.075
Occupancy	0.239	0.157

E. Results and Discussions on Estimation of Traffic Variables

Here, we assess the proposed algorithm in terms of its accuracy in estimating flow and occupancy using MAPE, which is used to assess the relative size of the estimation errors as shown in (5), where $\hat{y}_{x_0,l_0,n}$ is the estimated traffic variable at time n on lane l_0 at the target site x_0. The traffic variable $y_{x_0,l_0,n}$ at time n on lane l_0 is obtained from the camera at the target site x_0, and M denotes the total number of estimated points, i.e.,

$$\text{MAPE} = \frac{1}{M}\sum_{n=1}^{M}\left|\frac{\hat{y}_{x_0,l_0,n} - y_{x_0,l_0,n}}{y_{x_0,l_0,n}}\right|. \tag{5}$$

Table I shows MAPE collectively calculated from using the proposed algorithm, the three-detector algorithm, KF-1 and KF-2 to estimate traffic variables every 5 mins, in the testing set under different traffic conditions at different times of day. We

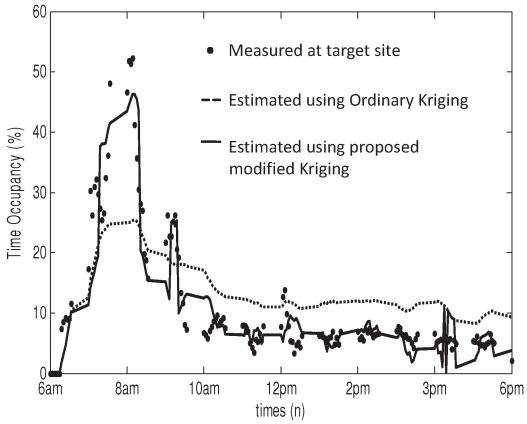

Fig. 9. Estimation of 5 mins occupancy on the shoulder lane at the target site. Transient anomaly was recorded at 9:25–9:45 A.M. on October 12, 2009.

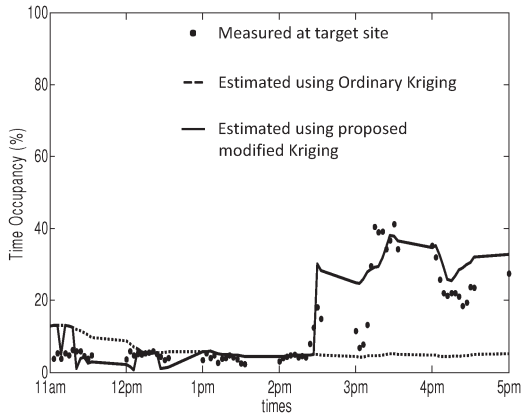

Fig. 10. Estimation of 5 mins occupancy on the shoulder lane at the target site. Lane blocking was recorded at 2:30 P.M. on October 18, 2009.

note that as the three-detector algorithm is designed primarily to estimate traffic flow, only the estimation results of traffic flow are shown.

It can be seen from Table I that the proposed algorithm achieves lower MAPEs than the three-detector algorithm and KF-1. With respect to the three-detector algorithm, most estimation errors correspond to the periods when travel time diverted from the expected wave propagation models (e.g., very light traffic or a lane blocking on the segment) and caused large spatial variability between the target site and upstream–downstream measurement sites. For example, a lane blocking caused some vehicles to travel longer than anticipated and, subsequently, the overestimation of flow at the target site. Unlike the three-detector algorithm, the proposed algorithm uses concurrent measurements of both upstream–downstream variability [$C_{l_0,l_1,n}$ in (1)] and lane-level variability [$\rho_{l_0,n}$ in (2)], which can capture changes in spatial variability as described in Section V-B.

Moreover, from Table I, we can see that the proposed algorithm outperforms KF-1 on the median lane because the median lane is usually a faster and a more dynamic lane on the expressway segment analyzed. It is observed that on the median lane, vehicles usually have more room to maneuver, which subsequently increases the likelihood that the traffic variables measured at the target site are significantly different from measurement sites. The proposed algorithm incorporates the variation between these upstream and downstream traffic variables, which copes better with changes at the target site.

KF-2 has the least amount of error because it is evaluated under an ideal scenario and, hence, is included as a benchmark where data from the target site can be used for estimation. Table I shows that the proposed algorithm performs very well as its MAPEs are much closer to those of KF-2 than the MAPEs of the three-detector and KF-1.

Figs. 9 and 10 show the online estimation capabilities of the proposed algorithm. In Fig. 9, the online estimation responds well to a temporary increase in occupancy due to transient anomaly from approximately 9:25 A.M. to 9:45 A.M.. Furthermore, the proposed algorithm can estimate abrupt increase in occupancy at the target site at approximately 2:30 P.M., as shown in Fig. 10. This is followed by a sudden decrease at 3 P.M., an increase at 3:20 P.M., and another decrease at 4:00 P.M. of occupancy. Considering that local traffic variables at the target site are not used at all, the trend of the estimated values in Fig. 10 still shows the ability of the proposed algorithm to respond to these changes. Furthermore, Figs. 9 and 10 show that incorporating spatial variability with weighting factors [second term in (3)] significantly enhances the estimation accuracy compared with using ordinary kriging alone. Particularly, the weighted spatial variability plays an essential role when there is a significant spatial difference due to a lane blocking (after 2:30 P.M. in Fig. 10).

TABLE II
MAPE FROM ESTIMATING AGGREGATE FLOW

Experimental Periods	Proposed Algorithm	Three-detector Algorithm
Weekday 7:00-9:00AM	0.119	0.368
Weekend 7:00-9:00AM	0.307	0.796

Table II shows experimental comparisons with the three-detector algorithm for aggregate flow estimation between 7:00 A.M. and 9:00 A.M. where traffic is heavy during rush hours on weekdays and light on weekends. It is found that the two experimental periods have high spatial variability between the target and upstream–downstream measurement sites. This subsequently causes high MAPEs for the three-detector algorithm as there is higher variability than anticipated in its wave propagation models. In contrast, the proposed algorithm shows lower MAPEs because the estimation model's parameters can be adjusted according to spatial variability between measurement sites.

We also assess the proposed algorithm under different temporal and spatial aggregations. Table III shows that MAPEs can be reduced by using smaller time aggregation periods, whereas Table IV compares MAPEs when the proposed algorithm is used to estimate lane-level and aggregate traffic flow. It can be seen that the proposed algorithm can be used for both aggregate and lane-level estimation with similar accuracy.

We further evaluate the proposed algorithm on an NGSIM US-101 data set [16]. Two virtual sensors are placed upstream and downstream of the target segment to calculate input traffic variables [31], and we assess the algorithm by placing a virtual sensor at the middle of the segment (the target site). The 7:50–8:20 A.M.: Lane1 data set (approximately two thirds of

TABLE III
MAPE FROM ESTIMATING TRAFFIC VARIABLES UNDER DIFFERENT TIME AGGREGATION PERIODS

Flow Estimation (Time Aggregation Periods)	MAPE on Shoulder Lane	MAPE on Median Lane
5 mins	0.230	0.148
2 mins	0.240	0.135
1 min	0.180	0.112
Occupancy Estimation (Time Aggregation Periods)	MAPE on Shoulder Lane	MAPE on Median Lane
5 mins	0.463	0.241
2 mins	0.464	0.238
1 min	0.423	0.210

TABLE IV
MAPE FROM ESTIMATING LANE-LEVEL AND AGGREGATE TRAFFIC FLOW

Time Aggregation Periods Periods	Lane-level MAPE	Aggregate MAPE
5 mins	0.230	0.262
2 mins	0.240	0.237
1 min	0.180	0.218

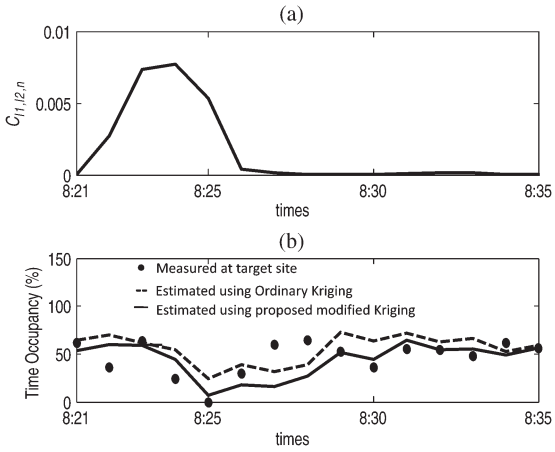

Fig. 11. Assessing the proposed algorithm using NGSIM's US-101:08:20–08:35 A.M.: Lane 1. (a) Inference of traffic transition. (b) Estimation of 1 min occupancy.

the data) is used for training and 8:20–8:35 A.M.: Lane1 data set (approximately one third of the data) is used for testing. The obtained inference rule is similar to that shown in Section V-B; however, due to high volume of vehicles, the upper bound of the weighting factor for occupancy estimation under the congested condition is reduced to $a_{l_0,n} = min(\rho_{l_0,n}, 0.5)$.

As shown in Fig. 11(a), the spatial covariance $(C_{l_1,l_2,n})$ is always lower than 0.5 (see Section V-B); hence, the proposed algorithm rightly infers a congested condition. Fig. 11(b) shows the capability of the proposed algorithm for online estimation of 1 min occupancy at the target site. It can be seen that the proposed algorithm, which incorporates spatial variability, responds generally well to changes in occupancy compared with using ordinary kriging alone. The only exceptions are at 8:27 A.M. and 8:28 A.M., where there is a delay in responding to a sudden increase in occupancy. Nevertheless, the proposed algorithm can again adjust to this change at 8:29 A.M.. This delay can be reduced by incorporating a model to capture patterns of occupancy drop into (3), which is worth further investigating.

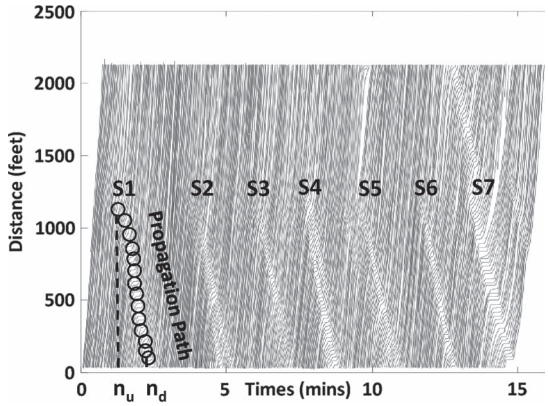

Fig. 12. Trajectory plot of NGSIM US-101:07:50–08:05 A.M.: Lane1 data with shockwave fronts $S1 - S7$.

F. Results and Discussions on Shockwave Propagation Time Estimation

For this test, we use NGSIM's US-101 data set [16] to estimate the shockwave propagation time. As shown in Fig. 12, if vehicle trajectory information is available, propagation paths of shockwave fronts $S1 - S7$ can be identified, and $S1$'s propagation time can be simply estimated as $n_d - n_u$. However, such detailed information would require every vehicle to be equipped with automatic vehicle location technologies or sensors with coverage of the entire road segment, which may yet to be available on many roadways. Note that the proposed algorithm does not require vehicle trajectory information as it uses only traffic information from upstream and downstream measurement sites.

Once a congested condition is inferred, the proposed algorithm can further estimate the shockwave propagation time using 7:50–8:05 A.M.: Lane1 data set as shown in Fig. 12. A sliding window L of 5 mins is used where time series of 30-s average local traffic speeds from the upstream and downstream virtual sensors are used as inputs. In each sliding window, the proposed algorithm assesses different time lags $\{\tau : 0 \leq \tau \leq 600 \text{ s}\}$ by comparing their corresponding LoCo scores in (4). Recall that the shockwave propagation is estimated as the time lag that gives maximum LoCo scores.

Using the proposed algorithm, propagation times of $S1 - S7$ in Fig. 12 are estimated to be {90, 75, 45, 30, 105, 75, 150} s, respectively. As the distance between sensors is known, these propagation times are then used to calculate backward velocities of shockwaves' fronts. These propagation times give an average shockwave velocity of approximately 18.27 km/h, which is very close to the average velocity reported in previous studies [23], [32], [33]. We note that unlike previously proposed methods, the proposed algorithm can estimate shockwave propagation time online.

VI. FINAL REMARKS

This paper proposes an online algorithm with three primary objectives: 1) to spatially infer traffic transitions at the target site where local traffic measurements cannot be obtained directly; 2) to estimate flow and occupancy at lane-level at the same target site; and 3) to estimate lane-level shockwave propagation times online.

The performance evaluations are conducted using a real-world data set measured from a road segment in Bangkok and the NGSIM US-101 data set [16]. With respect to inferring traffic transitions, the proposed algorithm outperforms the previously proposed dual-station algorithm [3] under low-flow conditions. When estimating traffic variables where local measurements are missing, the proposed algorithm acheives lower estimation errors than the three-detector and KF-based algorithms [1], [4], [8]. Finally, the proposed algorithm can well estimate lane-level shockwave propagation times online, which can provide further information, e.g., monitoring evolution of shockwave for online variable speed limit control [26].

The encouraging results obtained in this paper grant further investigation to improve the estimation accuracy by incorporating more spatiotemporal characteristics. Combining concurrent spatial variability of the proposed algorithm with the wave propagation models of the three-detector algorithm [1], [2] should also significantly improve the estimation accuracy. Moreover, incorporating algorithms in [12] and [13] that detect and classify traffic anomalies at the sensors' locations would enhance the classification and positioning of traffic disruptions, which can provide more information for traffic management center personnel. Finally, the extension to segment with more than two lanes is worth investigating. In this case, the spatial covariance matrix should first be constructed from spatial covariances of each pair of adjacent lanes. As the system grows in dimensionality, the largest eigenvalue of the covariance matrix can be used instead of individual spatial covariances to infer traffic transition. This approach should also be applicable to other geometries of road segments as long as historical traffic data are available for analysis and calibration.

ACKNOWLEDGMENT

The authors would like to thank Dr. E. Garcia-Trevino of the ISN group, Imperial College London for the useful discussions and Dr. Supakorn, Dr. Suporn, and Mr. Chaiyapoom from NECTEC, Thailand for their assistance in providing data for the analysis. The authors would also like to thank the anonymous reviewers for their useful and important comments for improving this paper and future investigations.

REFERENCES

[1] W. Deng and X. Zhou, "Freeway traffic state estimation and uncertainty quantification based on heterogeneous data sources: Stochastic three-detector approach," presented at the Proc. Transp. Res. Board Nat. Academies, Washington, DC, USA, 2012, 12-0710, [CD-ROM].

[2] G. Newell, "A simplified theory of kinematic waves in highway traffic Part I: General theory," *Transp. Res. Part B, Methodological*, vol. 27, no. 4, pp. 281–287, Aug. 1993.

[3] H. Fan and L. M. Chin, "Development of dual-station automated expressway incident detection algorithms," *IEEE Trans. Intell. Transp. Syst.*, vol. 8, no. 3, pp. 480–490, Sep. 2007.

[4] B. Ghosh, B. Basu, and M. O'Mahony, "Multivariate short-term traffic flow forecasting using time-series analysis," *IEEE Trans. Intell. Transp. Syst.*, vol. 10, no. 22, pp. 246–254, Jun. 2009.

[5] E. I. Vlahogianni, J. C. Golias, and M. G. Karlaftis, "Short-term traffic forecasting: Overview of objectives and methods," *Trans. Rev.*, vol. 24, no. 5, pp. 533–557, Sep. 2004.

[6] M. Lippi, M. Bertini, and P. Frasconi, "Short-term traffic flow forecasting: An experimental comparison of time-series analysis and supervised learning," *IEEE Trans. Intell. Transp. Syst.*, vol. 14, no. 2, pp. 871–882, Jun. 2013.

[7] C. Chen, Z. Liu, W. Lin, S. Li, and K. Wang, "Distributed modeling in a MapReduce framework for data-driven traffic flow forecasting," *IEEE Trans. Intell. Transp. Syst.*, vol. 14, no. 1, pp. 22–33, Mar. 2013.

[8] Y. Wang *et al.*, "Real-time freeway network traffic surveillance: Large-scale field-testing results in Southern Italy," *IEEE Trans. Intell. Transp. Syst.*, vol. 12, no. 2, pp. 548–562, Jun. 2011.

[9] P. Raphiphan, A. Zaslavsky, P. Prathombutr, and P. Meesad, "Context aware traffic congestion estimation to compensate intermittently available mobile sensors," in *Proc. 10th Int. Conf. Mobile Data Manag., Syst., Serv. Middleware*, 2009, pp. 405–410.

[10] H. Braxmeier, V. Schmidt, and E. Spodarev, "Spatial extrapolation of anisotropic road traffic data," *Image Anal Sterology*, vol. 23, no. 3, pp. 185–198, 2004.

[11] X. Wang and K. M. Kockelman, "Forecasting network data: Spatial interpolation of traffic counts from Texas data," *Transp. Res. Rec., J. Transp. Res. Board*, vol. 2105, pp. 100–108, 2009, 09-2294.

[12] J. A. Barria and S. Thajchayapong, "Detection and classification of traffic anomalies using microscopic traffic variables," *IEEE Trans. Intell. Transp. Syst.*, vol. 12, no. 3, pp. 695–704, Sep. 2011.

[13] S. Thajchayapong, E. S. Garcia-Trevino, and J. A. Barria, "Distributed classification of traffic anomalies using microscopic traffic variables," *IEEE Trans. Intell. Transp. Syst.*, vol. 14, no. 1, pp. 448–458, Mar. 2013.

[14] V. Hurdle and B. Son, "Road test of a freeway model," *Transp. Res. Part A, Policy Practice*, vol. 34, no. 7, pp. 537–564, Sep. 2000.

[15] B. Coifman and Y. Wang, "Average velocity of waves propagating through congested freeway traffic," in *Proc. 16th Int. Symp. Transp. Traffic Theory*, 2005, pp. 165–179.

[16] V. Alexiadis, J. Colyar, J. Halkias, R. Hranac, and G. McHale, "The next generation simulation program," *ITE Journal*, vol. 74, no. 8, pp. 22–26, 2004.

[17] K. Kiratiratanapruk and S. Siddhichai, "Vehicle detection and tracking for traffic monitoring system," in *Proc. IEEE TENCON*, Nov. 2006, pp. 1–4.

[18] S. Thajchayapong, J. A. Barria, and E. Garcia-Trevino, "Lane-level traffic estimations using microscopic traffic variables," in *Proc. 13th IEEE Int. Conf. Intell. Transp. Syst.*, 2010, pp. 1189–1194.

[19] R. Weil, J. Wooton, and A. Garcia-Ortiz, "Traffic incident detection: Sensors and algorithms," *Mathematical and Computing Modelling*, vol. 27, no. 9–11, pp. 257–291, May/Jun. 1998.

[20] N. Marinica, A. Sarlette, and R. K. Boel, "Distributed particle filter for urban traffic networks using a platoon-based model," *IEEE Trans. Intell. Transp. Syst.*, vol. 14, no. 4, pp. 1918–1929, Dec. 2013.

[21] Y. Yuan, J. V. Lint, R. Wilson, F. van Wageningen-Kessels, and S. Hoogendoorn, "Real-time Lagrangian traffic state estimator for freeways," *IEEE Trans. Intell. Transp. Syst.*, vol. 13, no. 1, pp. 59–70, Mar. 2012.

[22] H. Wackernagel, *Multivariate Geostatistics*. Berlin, Germany: Springer-Verlag, 1998.

[23] N. Chiabaut, C. Buisson, and L. Leclercq, "Fundamental diagram estimation through passing rate measurements in congestion," *IEEE Trans. Intell. Transp. Syst.*, vol. 10, no. 2, pp. 355–359, May 2009.

[24] *Highway Capacity Manual*, Transportation Research Board, Washington, DC, USA, 2000.

[25] L. C. Edie, "Discussion of traffic stream measurements and definitions," in *Proc. Int. Symp. Transp. Traffic Theory*, 1965, pp. 139–154.

[26] A. Hegyi, B. D. Schutter, and J. Hellendoorn, "Optimal coordination of variable speed limits to suppress shock waves," *IEEE Trans. Intell. Transp. Syst.*, vol. 6, no. 1, pp. 102–112, Mar. 2005.

[27] W. Cohen, "Fast effective rule induction," in *Proc. 12th Int. Conf. Mach. Learning*, 1995, pp. 115–123.

[28] M. Cassidy, "Bivariate relations in nearly stationary highway traffic," *Transp. Res. Part B, Methodological*, vol. 32, no. 1, pp. 49–59, Jan. 1998.

[29] S. Papadimitriou, J. Sun, and P. Yu, "Local correlation tracking in time series," in *Proc. 6th Int. Conf. Data Mining*, 2006, pp. 456–465.

[30] I. Okutani and Y. J. Stephanedes, "Dynamic prediction of traffic volume through Kalman filtering theory," *Transp. Res. Part B*, no. 18, pp. 1–11, Feb. 1984.

[31] L. Li, X. Chen, Z. Li, and L. Zhang, "Freeway travel-time estimation based on temporal–spatial queueing model," *IEEE Trans. Intell. Transp. Syst.*, vol. 14, no. 3, pp. 1536–1541, Sep. 2013.

[32] N. Chiabaut, L. Leclercq, and C. Buisson, "From heterogeneous drivers to macroscopic patterns in congestion," *Transp. Res. Part B, Methodological*, vol. 44, no. 2, pp. 299–308, Feb. 2010.

[33] X. Lu and A. Skabardonis, "Freeway traffic shockwave analysis: Exploring NGSIM trajectory data," presented at the Proc. Transp. Res. Board Nat. Academies, Washington, DC, USA, 2007, 07-3016, [CD-ROM].

Suttipong Thajchayapong received the M.S. and B.S. degrees in electrical and computer engineering from Carnegie Mellon University, Pittsburgh, PA, USA, and the Ph.D. degree in electrical and electronic engineering from Imperial College London, London, U.K.

He is a Researcher with National Electronic and Computer Technology Centre, National Science and Technology Development Agency, Pathumthani, Thailand. His research interests include intelligent transportation systems with emphasis on vehicular traffic monitoring and simulation, anomaly detection, and mobility and quality of service in wireless networks.

Dr. Thajchayapong is a Member of ITS Thailand.

Javier A. Barria (M'02) received the Ph.D. degree in electrical and electronic engineering and the M.B.A. degree from Imperial College London, London, U.K., in 1994 and 1997, respectively.

He is a Reader with the Intelligent Systems and Networks Group, Department of Electrical and Electronic Engineering, Imperial College London. His research interests include network monitoring strategies, anomaly detection, and network performance estimation for wireless sensor networks and intelligent transportation systems.

Dr. Barria is a Fellow of the Institution of Engineering and Technology and a Chartered Engineer in the U.K. He was a British Telecom Research Fellow from 2001 to 2002.